discriminate the cationic ACh from analogous neutral molecules through a stabilizing cation-π interaction.

REFERENCES AND NOTES

1. Acetylcholine binds to esterases with K_d of ~1 mM (2). At the McPC603 binding site, K_d is ~10 μM for phosphocholine, and 1 mM for choline (3). Binding to the ACh receptors is complex, involving two positively cooperative, nonequivalent sites, and at least four functional states in the nicotinic AChR. The value of K_d obtained depends on the type of measurement being made. Dose-response curves characterize a low-affinity conformation of the nAChR (50 to 100 μM) associated with the resting state. Equilibrium binding studies identify a high-affinity conformation (~3 nM) associated with desensitized states. See (4) for further discussions.
2. F. B. Hasan, S. G. Cohen, J. B. Cohen, *J. Biol. Chem.* **255**, 3898 (1980); F. B. Hasan, J. L. Elkind, S. G. Cohen, J. B. Cohen, *ibid.* **256**, 7781 (1981); S. G. Cohen, D. L. Lieberman, F. B. Hasan, J. B. Cohen, *ibid.* **257**, 14087 (1982).
3. Y. Satow, G. H. Cohen, E. A. Padlan, D. R. Davies, *J. Mol. Biol.* **190**, 593 (1986); P. Gettins, M. Potter, R. J. Leatherbarrow, R. A. Dwek, *Biochemistry* **21**, 4927 (1982); E. D. Getzoff, J. A. Tainer, R. A. Lerner, H. M. Geysen, *Adv. Immunol.* **43**, 1 (1988); P. G. Schultz, *Science* **240**, 426 (1988).
4. E. L. M. Ochoa, A. Chattopadhyay, M. G. McNamee, *Cell. Mol. Neurobiol.* **9**, 141 (1989); A. Karlin, in *The Cell Surface and Neuronal Function*, C. W. Cotman, G. Poste, G. L. Nicolson, Eds. (Elsevier/North Holland Biomedical, Amsterdam, 1980), pp. 191–260.
5. The steric fit between **1** and ACh is not optimal. Other cationic guests that are better suited to the dimensions of the cavity of **1** show K_d values of ~1 μM (6).
6. T. J. Shepodd, M. A. Petti, D. A. Dougherty, *J. Am. Chem. Soc.* **108**, 6085 (1986); *ibid.* **110**, 1983 (1988); M. A. Petti, T. J. Shepodd, R. E. Barrans, Jr., D. A. Dougherty, *ibid.*, p. 6825; D. A. Stauffer and D. A. Dougherty, *Tetrahedron Lett.* **29**, 6039 (1988); D. A. Stauffer, R. E. Barrans, Jr., D. A. Dougherty, *Angew. Chem. Int. Ed. Engl.* **29**, 915 (1990).
7. Conditions and methods for determining the K_d for ACh were as in previous studies (6).
8. Such stabilizing interactions have been seen in the gas phase [M. Meot-Ner (Mautner) and C. A. Deakyne, *J. Am. Chem. Soc.* **107**, 469 (1985); C. A. Deakyne and M. Meot-Ner (Mautner), *ibid.*, p. 474] and are similar to the interaction of protonated amines with aromatic residues seen in many protein structures [S. K. Burley and G. A. Petsko, *FEBS Lett.* **203**, 139 (1986)].
9. There is a strong enthalpic component to the cation binding, consistent with an attractive cation-π interaction, in contrast to solvent repulsion (hydrophobic) forces; see D. A. Stauffer, R. E. Barrans, Jr., D. A. Dougherty, *J. Org. Chem.* **55**, 2762 (1990).
10. A. McCurdy and D. A. Dougherty, unpublished results.
11. L. Mizoue and D. A. Dougherty, unpublished results.
12. M. Dhaenens, L. Lacombe, J.-M. Lehn, J.-P. Vigneron, *J. Chem. Soc. Chem. Commun.* **1984**, 1097 (1984).
13. H.-J. Schneider, D. Güttes, U. Schneider, *J. Am. Chem. Soc.* **110**, 6449 (1988).
14. R. W. Zwanzig, *J. Chem. Phys.* **22**, 1420 (1954).
15. W. L. Jorgensen, *Acc. Chem. Res.* **22**, 184 (1989).
16. P. A. Bash, U. C. Singh, F. K. Brown, R. Langridge, P. A. Kollman, *Science* **236**, 564 (1987).
17. Calculations used the program BOSS (version 2.7; W. L. Jorgensen) and included TIP4P water and standard OPLS parameters (15) augmented with parameters for the aromatic ring based on appropriate AM1 (18) calculations.
18. M. J. S. Dewar, E. G. Zoebisch, E. F. Healy, J. J. P. Stewart, *J. Am. Chem. Soc.* **107**, 3902 (1985).
19. For related calculations, see B. G. Rao and U. C. Singh, *ibid.* **111**, 3125 (1989).
20. See, for example, A. D. Elbeiu, in *Comprehensive Medicinal Chemistry*, P. G. Sammes, Ed. (Pergamon, Oxford, 1990), vol. 2, pp. 365–389.
21. B. Kieffer, M. Goeldner, C. Hirth, R. Aebersold, J.-Y. Chang, *FEBS Lett.* **202**, 91 (1986).
22. J.-L. Sikorav, E. Krejci, J. Massoulié, *EMBO J.* **6**, 1865 (1987).
23. Expanding the sequences in *Torpedo* and *Drosophila*, one finds anionic residues (Glu and Asp) three and four residues toward the amino terminus from the X residue, and a Tyr four residues toward the carboxyl terminus.
24. For recent reviews, see W. H. M. L. Luyten, *J. Neurosci. Res.* **16**, 51 (1986); A. Maelicke, Ed., *Nicotinic Acetylcholine Receptor: Structure and Function* (Springer-Verlag, Berlin, 1986).
25. P. N. Kao *et al.*, *J. Biol. Chem.* **259**, 11662 (1984).
26. M. Dennis *et al.*, *Biochemistry* **27**, 2346 (1988).
27. J.-L. Galzi *et al.*, *J. Biol. Chem.* **265**, 10430 (1990).
28. F. M. Menger, D. S. Davis, R. A. Persichetti, J.-J. Lee, *J. Am. Chem. Soc.* **112**, 2451 (1990).
29. See, for example, P. R. Cullis and M. J. Hope, in *Biochemistry of Lipids and Membranes*, D. E. Vance and J. E. Vance, Eds. (Benjamin/Cummings, Menlo Park, CA, 1985), pp. 25–72.
30. We note, for example, the prominent role of Phe in small peptides that inhibit fusion of Sendai virus with cells. See, for example, C. D. Richardson, A. Scherd, P. W. Choppin, *Virology* **105**, 205 (1980).
31. J. Novotny, R. E. Bruccoleri, F. A. Saul, *Biochemistry* **28**, 4735 (1989).
32. Note that essentially all of the charge of a tetraalkylammonium ion resides on the CH_2 and CH_3 groups attached to nitrogen, not on the nitrogen.

33. Supported by the Office of Naval Research (N000014-88-K-0259) and the National Institutes of Health (GM36356 and GM43936). We thank H. Lester and A. Karlin for helpful discussions and W. L. Jorgensen for providing a copy of the program BOSS. Contribution no. 8174 from the Division of Chemistry and Chemical Engineering, California Institute of Technology.

17 July 1990; accepted 11 September 1990

Crystal Structure of Cobra-Venom Phospholipase A_2 in a Complex with a Transition-State Analogue

Steven P. White, David L. Scott, Zbyszek Otwinowski, Michael H. Gelb, Paul B. Sigler

The crystal structure of a complex between a phosphonate transition-state analogue and the phospholipase A_2 (PLA_2) from *Naja naja atra* venom has been solved and refined to a resolution of 2.0 angstroms. The identical stereochemistry of the two complexes that comprise the crystal's asymmetric unit indicates both the manner in which the transition state is stabilized and how the hydrophobic fatty acyl chains of the substrate are accommodated by the enzyme during interfacial catalysis. The critical features that suggest the chemistry of binding and catalysis are the same as those seen in the crystal structure of a similar complex formed with the evolutionarily distant bee-venom PLA_2.

Phospholipase A_2 (PLA_2) hydrolyzes the *sn-2* ester of phospholipids, preferably in lamellar or micellar aggregates. Special interest in the mechanism of PLA_2 action stems from its role as a paradigm for understanding calcium-mediated enzymatic events at the surface of membranes, especially those that release arachidonate and other second messengers (*1*).

In this report, we describe the crystal structure of a complex formed by PLA_2 from the venom of an elapid snake (*N. n. atra*) and a transition-state analogue (Fig. 1). The analogue, *L*-1-*O*-octyl-2-heptylphosphonyl-*sn*-glycero-3-phosphoethanolamine [figure 1 of (*2*)], was designed to emulate the tetrahedral transition state formed in the hydrolysis of dioctanoyl phosphatidylethanolamine and therefore is designated diC_8(2Ph)PE.

S. P. White, D. L. Scott, Z. Otwinowski, and P. B. Sigler, Department of Molecular Biophysics and Biochemistry and the Howard Hughes Medical Institute, Yale University, New Haven, CT 06511.
M. H. Gelb, Departments of Chemistry and Biochemistry, University of Washington, Seattle, WA 98195.

The two molecules in the crystallographic asymmetric unit chosen for refinement form a poorly stabilized dimer related by a rotation of 179.6° and a translation of 0.6 Å along the rotation axis. The bound transition-state analogue does not contribute in any obvious way to the stability of the dimer. Moreover, from the orientation of the inhibitor's *sn-1* and *sn-2* substituents, it is highly unlikely that both of this dimer's active sites can simultaneously interact with the same substrate aggregate. Thus, the architecture of this dimer provides no support for the notion that substrate-induced enzyme aggregation plays a role in PLA_2 catalysis (*3*).

When the α-carbon backbone trace of the PLA_2 from the venom of *N. n. atra* is contrasted with those of the enzymes from bovine pancreas (monomeric) (*4*) and the venom of *Agkistridon piscivorus piscivorus* (dimeric) (*5*), the elapid enzyme shows strong conservation of the homologous core [root-mean-square (rms) differences of 0.99 Å and 1.04 Å, respectively] (*6*). The conformation of the noncore backbone of the Class I *N. n.*

atra PLA_2 is more similar to that of the Class I bovine enzyme (rms difference = 2.0 Å) than to that of the Class II *A. p. piscivorus* (rms difference = 3.0 Å).

The electron density for both molecules of the asymmetric unit, as well as for the crystal structure of the uninhibited enzyme (*7*), indicates that the sequence of the isoform used to grow these crystals differs slightly from the published one (Fig. 2) (*8*).

One molecule of $diC_8(2Ph)PE$ is bound to each enzyme molecule at full occupancy and the position of the inhibitor's atoms are well defined (Fig. 3). Two trends are noted. The *sn-1* substituent is less firmly fixed than the *sn-2*, and the methylene and methyl groups furthest from the glycerol are the least well ordered. On the other hand, the conformation of the glycerol backbone and its substituents, as well as their relation to the catalytic residues and the calcium ion, are virtually the same in both molecules of the asymmetric unit.

The inhibitor's ethanolamine, a group commonly found esterified to the *sn-3* phosphate of naturally occurring neutral membrane phospholipids, forms a hydrogen bond through its primary amine with the side chain of the poorly conserved Asn53. This interaction is denied to the quaternary ammonium group of the more prevalent lecithin analogues. This contact is not likely to completely explain the impact of the distal *sn-3* ester on substrate specificity since the nature of the phosphoryl ester could also have a significant effect on the surface charge-potential distribution and other physical properties of the substrate aggregate.

	1 5 10 15 20 25 ■ ■30 ■
BOVINE	A L W Q F N G M I K C K I P S S E P L L D F N N Y G C Y C G L G G S
NNA	N * Y * * K N * * Q * T V * * R S - W W * * A D * * * * * * R * * *
APD	D * M * * E T L * M K I A K - R D G M F W Y S A * * * * * * W * * H
	35 40 45 ● ■ 50 □ 55 60 65
BOVINE	G T P V D D L D R C C Q T **H** **D** N C **Y** K Q A K K L D S C K V L V D N P Y
NNA	* * * * * * * * * * * * V * * * * * N E * E * I S G * - - - - - - W * *
APD	* L * Q * A T * * * * F V * * C * * G K V T - - G - * - - - - - - D * K
	70 75 80 85 90 95 ● 100
BOVINE	T N N Y S Y S C S N N E I T C S S E N N A C G A F I C N C **D** R N A A I
NNA	F K T * * * E * * Q G T L * * K G G * * - * A * A V * D * * * L * * *
APD	L D S * T * * V E * G D V V * - G G * * P * K K E * * E * * * A * * *
	105 110 115 120 125 130
BOVINE	C F S K V - P - Y N K E H K N L D K - K N C
NNA	* * A G A - * - * * D N D Y * I N L K A R * *Q E*
APD	* * R D N K V T * D N K Y W R F P P - Q N * K E E S E P C

Fig. 2. Comparison of the PLA_2 from *N. n. atra* venom and the PLA_2's from bovine pancreas and *Agkistridon piscivorus piscivorus* venom. Representative sequences of the Class I/II superfamily (*23*). Top row: bovine pancreatic (Class I) (*6*); middle row: *N. n. atra* venom (Class I) (*8*); bottom row: dimeric *A. p. piscivorus* (Class II) (*6*). They are arranged according to three-dimensional structural "homology" (*6*). Bold face indicates functionally critical residues: (●), catalytic; (■), calcium binding; and (□), invariant supporting tyrosine of catalytic network. Parentheses denote positions where the crystal structure disagrees with the published sequence (*8*); Ala90 is present in the crystal structure, and the two carboxyl-terminal residues are absent.

The alkane chains of the inhibitor's *sn-1* and *sn-2* substituents lie roughly parallel in a hydrophobic channel that extends approximately 14 Å from the catalytic site (His48-Nδ1) to its opening just "above" the amino-terminal helix (Fig. 4). The *sn-2* substituent is sharply bent at the tetrahedral phosphonate in a manner reminiscent of crystalline phospholipids [Fig. 3 and figure 1 of (*2*)] (*9*). The channel's surfaces are formed mainly by invariant or highly conserved hydrophobic residues. Looking into the channel (Fig. 5), the right wall of the channel is made by an invariant Ile9, and an invariant Phe5 provides the right side of the channel floor. Both contact the heptyl chain of the *sn-2* substituent. The left side of the channel floor is formed by the nearly invariant Leu2 (occasionally a Val) that contacts the *sn-1*-octyl chain. The roof of the channel is formed by Trp19, a position occupied by a hydrophobic residue in 85% of the known sequences. Finally, the left wall of the channel is formed by a potentially mobile hydrophobic "flap" that is secured firmly into place only after the substrate is productively bound. In the *N. n. atra* enzyme, this wall is the ring of Tyr69 whose phenolic hydroxyl is bound to the inhibitor's *sn-3* phosphate, which in turn is firmly anchored to the primary calcium ion. In all but one of the 53 sequences listed by van den Bergh *et al.* (*10*), the residue at position 69 is either a Tyr or Lys. Clearly, the role of Tyr69 can be assumed by Lys69 making use of the four methylene units of its side chain to form the hydrophobic left wall of the channel and its ε-amino group to bind to the *sn-3* phosphate. Thus, the productively bound phospholipid is "extracted" from the lamellar or micellar aggregate by a preferred diffusion pathway that maintains a hydrophobic environment for the fatty acyl groups and channels the scissile elements from the surface of the aggregate into the catalytic site. The polar groups can easily traverse this path, since the left wall of the hydrophobic channel is not completely formed by Tyr69 (or Lys69) until the *sn-3* phosphate has passed through the channel and is anchored to the calcium ion.

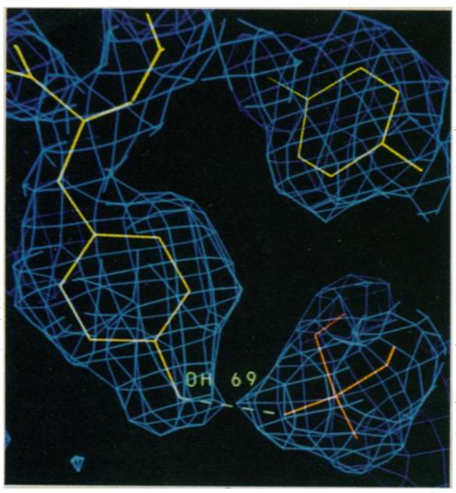

Fig. 1. Representative electron density of *N. n. atra* PLA_2 complexed with $diC_8(2Ph)PE$. Tyr69 forms a hydrogen bond with the *sn-3* phosphate of $diC_8(2Ph)PE$. The electron density is a $(2F_o-F_c)$ map (*17*). PLA_2 was isolated from the lyophilized venom (Miami Serpentarium) as described by Yuan *et al.* (*18*). It showed a single band on a silver-stained gel after electrophoresis in sodium dodecyl sulfate. Small (0.1 mm by 0.09 mm by 0.06 mm) crystals grew in 6 weeks from 20-μl droplets containing 10 mg/ml protein, 2 mM $diC_8(2Ph)PE$, 10 mM $CaCl_2$, 0.1 M tris, 0.7 M ammonium sulfate, pH 8.0, that were plated onto glass depression slides and sealed in boxes containing 20 ml of 1.4 M ammonium sulfate, 0.1 M tris, pH 8.0. The crystals were of space group $C222_1$, a = 34.6 Å, b = 73.5 Å, and c = 181.6 Å, with two molecules in the asymmetric unit. Data to 2.0 Å resolution (R_{sym} = 0.07) were collected with two San Diego Multiwire System detectors; source radiation was graphite-monochromated CuKα emission from an RU-300 x-ray generator. The structure was solved by molecular replacement (*19*) with the program Merlot 1.5 (*20*) modified to more accurately subtract the Patterson origin peak and to incorporate higher resolution terms. Bovine pancreatic PLA_2 (*4*), pruned of its non-homologous side chains, was used as the search structure. The initial electron-density map, phased with the pruned model, permitted fitting of many of the side chains that were not included in the search structure. Subsequent rounds of refinement with X-PLOR (*21*) and PROFFT (*22*) rapidly reduced the R factor while improving the stereochemistry. Refinement converged to an R factor of 0.179 for all data. On average, bond lengths, interbond angle distances, and planarities deviated less than 0.014, 0.029, and 0.038 Å from ideal values, respectively.

The enzyme's interfacial binding surface can be inferred from this structure. The extension of the alkyl chains from the surface marks the region where the enzyme contacts the substrate aggregate. This surface is not that described by Dijkstra *et al.* (*11*) but rather a surface that includes exposed residues in the first two turns of the amino terminal helix as well as those directly above the hydrophobic channel's opening (Figs. 4 and 5). This contact surface is consistent with the first half of the amino terminal helix and its immediate neighbors on the enzyme's surface being the focus of the structural changes that convert the pancreatic proenzyme into an enzyme and conferring upon the enzyme the ability to bind and rapidly hydrolyze aggregated, as opposed to soluble, substrate (*12*). It is also consistent with fluorescence studies which show that Trp3 of the pancreatic enzymes is desolvated upon binding to vesicles (*13*).

Calcium ion is essential for phospholipase activity. Two calcium ions are evident in each of the two molecules of the asymmetric unit. The "primary" site corresponds to the familiar location first noted in the bovine PLA_2 by Dijkstra *et al.* (*4*). Like most calcium ions that serve as functional cofactors (*14*), this calcium is hepta-coordinated in a pentangonal bipyramidal cage. In this case, the cage is composed of the carboxylate of the nearly invariant Asp49, the backbone carbonyls of the highly conserved "calcium-binding loop," and two O atoms of the inhibitor. In addition, there is a "secondary" site that is 6.6 Å from the primary site whose ligation cage is only penta-coordinated and is more loosely structured (*15*). This secondary site appears to replace a more typical seven-coordinated secondary site seen in the structure of the uninhibited form of the same enzyme (*2*). The functional role for this secondary calcium ion site is suggested in a companion article on mechanism (*2*). Figure 3 shows the stereochemical basis for the primary calcium ion's concerted role in both substrate binding and catalysis. One of the two axial ligands comes from the *sn-3* phosphate, and one of the five equatorial ligands comes from the *sn-2* phosphonate. The latter presumably simulates the stabilizing interaction between the electrophilic calcium ion and the oxyanion of the putative tetrahedral intermediate formed from the scissile ester's carbonyl group. This arrangement is similar to the corresponding site in the crystalline complex of the bee-venom PLA_2 inhibited with diC_8(2Ph)PE [figure 4 of (*7*)]. The two O atoms contributed by the inhibitor to the coordination shell of the calcium ion replace water molecules in the uninhibited form of the *N. n. atra* enzyme but leave the geometry unaltered. Thus, in productive-mode binding and during catalysis, the substrate appears to clamp the calcium ion in a stereospecific manner in which the *sn-3* phosphate interacts axially and the presumed oxyanion of the *sn-2* tetrahedral intermediate interacts equatorially. One non-bridging O atom of the phosphonate is perfectly situated to make a hydrogen bond with the protonated Nδ1 of His48. This oxygen corresponds to the position of the oxygen in a fixed water molecule first proposed by Verheij *et al.* (*16*) to be the attacking nucleophile in the bovine enzyme (*4*) and subsequently found to be hydrogen bonded to the active site His48 in every refined high-resolution crystal structure of PLA_2. Attack on the scissile carbonyl

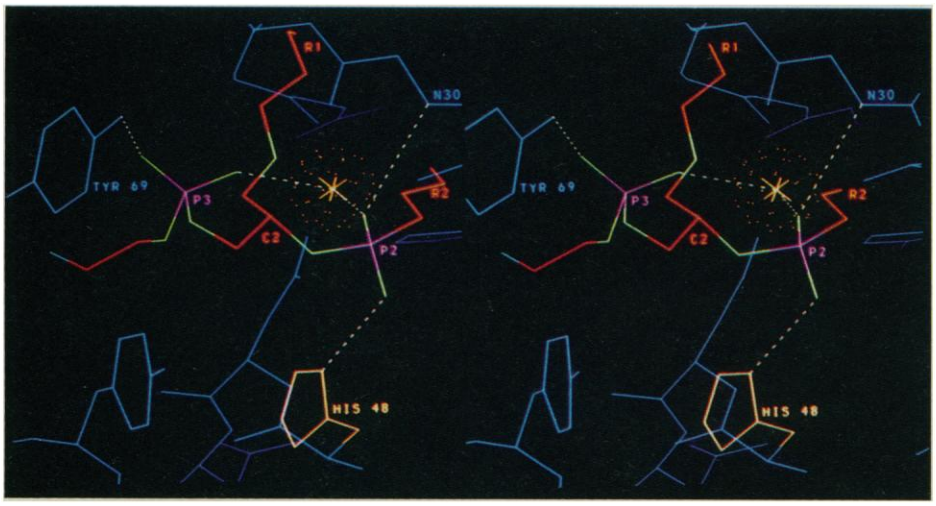

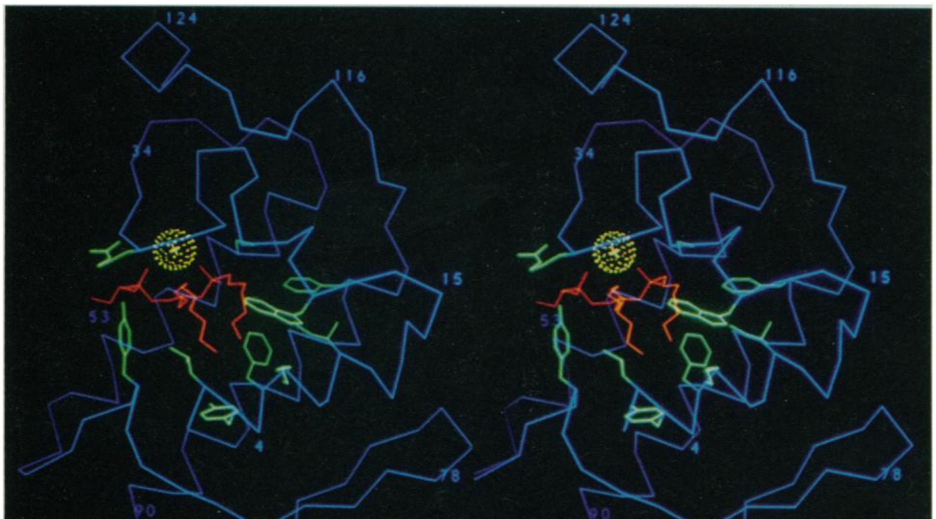

Fig. 3. (**Top**) Interaction of diC_8(2Ph)PE with the active site of *N. n. atra* PLA_2. Protein components are colored blue except for the gold side chain of the active site His48. The primary calcium ion is represented by the yellow sphere. In diC_8(2Ph)PE, the phosphorus atoms of the *sn-2* phosphonate (P2) and *sn-3* phosphate (P3) are magenta, oxygens are green, nitrogen is cyan, and the carbons are red. The termini of the *sn-1* (R1) and *sn-2* (R2) alkyl substituents are clipped off in this view. Tyr69 completes the hydrophobic channel by a stabilizing contact with the *sn-3* phosphate. The nonbridging oxygen of the *sn-3* phosphate that is coordinated by the principal calcium ion is also hydrogen bonded to N32 of the calcium-binding loop (bond not shown). **Fig. 4.** (**Bottom**) Complex of diC_8(2Ph)PE with the PLA_2 from *N. n. atra* venom. A Cα trace highlighting the calcium ion cofactor (yellow sphere), the diC_8(2Ph)PE inhibitor (red), side chains of the hydrophobic channel (green) [Leu(Val)2, Phe5, Tyr6, Ile9, and Trp19], and part of the interfacial binding surface (also in green) [Tyr(Trp)3, Lys6, and Arg 31].

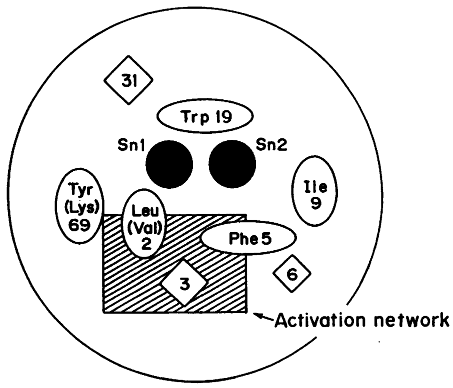

Fig. 5. The hydrophobic channel. A schematic display looking directly "into" the channel showing the residues that comprise the opening of the hydrophobic channel and are part of the presumed interfacial binding site of the *N. n. atra* enzyme. *Sn-1* and *sn-2* refer to the protruding termini of the alkyl substituents of diC_8(2Ph)PE. The diamonds indicate residues (shown in green in Fig. 4) whose side chains have been shown to be involved (3) or are likely to be involved (6 and 31) in interfacial binding.

by this universally present water molecule is presumably activated through the abstraction of a proton by the His48. A formal mechanism for PLA_2 catalysis has been advanced that is based on the stereochemistry described here (*2*) and in a parallel study on the inhibited bee-venom enzyme (*7*).

REFERENCES AND NOTES

1. J. Chang, J. H. Musser, H. McGregor, *Biochem. Pharmacol.* **36**, 2429 (1987); A. Achari *et al.*, *Cold Spring Harbor Symp. Quant. Biol.* **52**, 441 (1987); B. Samuelsson, *Drug* **33**, 2 (1987); _____, S.-E. Duhlen, J. Å. Lindgren, C. A. Rouzer, C. N. Serhan, *Science* **237**, 1171 (1987).
2. D. L. Scott *et al.*, *Science* **250**, 1541 (1990).
3. T. L. Hazlett and E. A. Dennis, *Biochim. Biophys. Acta* **961**, 22 (1988); A. G. Tomasselli *et al.*, *J. Biol. Chem.* **264**, 10041 (1989); W. Cho, A. G. Tomasselli, R. L. Heinrikson, F. J. Kezdy, *ibid.* **263**, 11237 (1988).
4. B. W. Dijkstra, K. H. Kalk, W. G. J. Hol, J. Drenth, *J. Mol. Biol.* **147**, 97 (1981).
5. D. L. Scott, A. Achari, S. Brunie, P. B. Sigler, in preparation.
6. R. Renetseder, S. Brunie, B. W. Dijkstra, J. Drenth, P. B. Sigler, *J. Biol. Chem.* **260**, 11627 (1985). The root mean square of a collection of N values x_i is $[(\Sigma x_i 2)/N]^{1/2}$. Here x_i is the distance between the ith pair of a set of N corresponding atoms after superimposition of two molecules or molecular segments. The program used was originally developed by A. Lesk.
7. D. L. Scott, Z. Otwinowski, M. H. Gelb, P. B. Sigler, *Science* **250**, 1563 (1990).
8. C. C. Yang, K. King, T. P. Sun, *Toxicon* **19**, 141 (1980).
9. M. Elder, P. Hitchcock, R. Mason, G. G. Shipley, *Proc. R. Soc. London Ser. A* **354**, 157 (1977); R. H. Pearson and I. Pascher, *Nature* **281**, 499 (1979); H. Hauser, I. Pascher, R. H. Pearson, S. Sundell, *Biochim. Biophys. Acta* **650**, 21 (1981).
10. C. J. van den Bergh, A. J. Slotboom, H. M. Verheij, G. H. de Haas, *J. Cell Biochem.* **39**, 379 (1989).
11. Although there is some overlap of the interfacial binding surface described by Dijkstra *et al.* [B. W. Dijkstra, J. Drenth, K. W. Kalk, *Nature* **289**, 604 (1981)] and that described here, the direction of the substrate's approach to the catalytic surface implicit in the description of Dijkstra *et al.* is nearly perpendicular to that suggested by the orientation of the bound substrate analogue.
12. J. P. Abita, M. Lazdunski, P. P. M. Bonsen, W. A. Pieterson, G. H. de Haas, *Eur. J. Biochem.* **30**, 37 (1972): M. A. Pieterson, J. J. Volwerk, G. H. de Haas, *Biochemistry* **13**, 1455 (1974).
13. M. K. Jain and W. L. C. Vaz, *Biochim. Biophys. Acta* **905**, 1 (1987); R. D. Ludescher *et al.*, *Biochemistry* **27**, 6618 (1988).
14. H. Einspahr and C. E. Bugg, in *Calcium Binding Proteins and Calcium Function*, R. H. Wasserman *et al.*, Eds. (Elsevier North-Holland, New York, 1977), pp. 13–19; A. Persechini, N. D. Moncrief, R. H. Kretsinger, *Trends Neurosci.* **12**, 462 (1989); M. N. G. James, *Annu. Rev. Biochem.* **58**, 951 (1989).
15. Calcium ions are identified by the refinement assigning a compact density of 18 electrons to the site with a temperature factor consistent with those of the surrounding atoms. Attempts to assign a water molecule to the same density caused the refinement to simulate an even more compact higher density by imposing a physically unrealistic negative temperature factor. There is no way to confidently distinguish a calcium from the isoelectronic potassium ion by x-ray crystallography; however, no potassium salts were used in the preparation or purification of the proteins, $diC_8(2Ph)PE$, or any of the crystal-stabilizing supernatant solutions.
16. H. M. Verheij *et al.*, *Biochemistry* **19**, 743 (1980).
17. The coefficients of the Fourier sum are $(2F_o - F_c)\exp(i\phi_c)$, where F_o is the observed amplitude and F_c and ϕ_c are the amplitude and phase, respectively, of the structure factors calculated from the refined model.
18. W. Yuan *et al.*, *Biochemistry* **29**, 6082 (1990).
19. R. A. Crowther, in *The Molecular Replacement Method*, M. G. Rossman, Ed. (Gordon and Breach, New York, 1972, pp. 173–178; R. A. Crowther and D. M. Blow, *Acta Crystallogr.* **23**, 544 (1967).
20. P. M. D. Fitzgerald, *J. Appl. Crystallogr.* **21**, 273 (1988).
21. A. T. Brünger, J. Kuriyan, M. Karplus, *Science* **235**, 458 (1987).
22. W. A. Hendrickson and J. H. Konnert, *Biomolecular Structure, Function, Conformation and Evolution*, R. Srinivasan, Ed. (Pergamon, Oxford, 1981), vol. 1, pp. 43–57.
23. Abbreviations for the amino acid residues are: A, Ala; C, Cys; D, Asp; E, Glu; F, Phe; G, Gly; H, His; I, Ile; K, Lys; L, Leu; M, Met; N, Asn; P, Pro; Q, Gln; R, Arg; S, Ser; T, Thr; V, Val; W, Trp; and Y, Tyr.

24. The research at Yale was supported by NIH grant GM22324 and by the Howard Hughes Medical Institute; the research at the University of Washington was supported by NIH grant HL 36235. S.P.W. is a fellow of the Arthritis Foundation, and D.L.S. is a postgraduate fellow at Yale.

4 June 1990; accepted 27 September 1990

Crystal Structure of Bee-Venom Phospholipase A_2 in a Complex with a Transition-State Analogue

DAVID L. SCOTT, ZBYSZEK OTWINOWSKI, MICHAEL H. GELB, PAUL B. SIGLER

The 2.0 angstroms crystal structure of a complex containing bee-venom phospholipase A_2 (PLA_2) and a phosphonate transition-state analogue was solved by multiple isomorphous replacement. The electron-density map is sufficiently detailed to visualize the proximal sugars of the enzyme's N-linked carbohydrate and a single molecule of the transition-state analogue bound to its active center. Although bee-venom PLA_2 does not belong to the large homologous Class I/II family that encompasses most other well-studied PLA_2s, there is segmental sequence similarity and conservation of many functional substructures. Comparison of the bee-venom enzyme with other phospholipase structures provides compelling evidence for a common catalytic mechanism.

PHOSPHOLIPASES A_2 (PLA_2, EC 3.1.1.4) specifically hydrolyze the 2-ester bond of *L*-glycerophospholipids. These enzymes have been purified from a variety of sources including mammalian pancreas, reptile and insect venoms, and synovial fluid. Since certain cellular forms of the enzyme may catalyze the release of arachidonate and thereby precipitate the inflammatory cascade, modulation of PLA_2 activity is of great pharmacological interest.

The amino acid sequences of the large homologous family of PLA_2s have been divided into two closely related structural classes, Class I (pancreatic juice and elapid venom) and Class II enzymes (crotalid and viper venoms) (*1*). The chemically determined sequence of the PLA_2 from the honeybee (*Apis mellifera*) (*2*) indicated that this enzyme was structurally distinct from the Class I/II superfamily. The amino acid sequence recently deduced from a cDNA clone differs from the chemically determined one, but both suggest that segments containing residues involved in calcium binding and catalysis are conserved (*3*, *4*). Bee-venom PLA_2, which is the principal allergen of bee venom, also differs from most other PLA_2s in that it contains an asparagine-linked oligosaccharide whose effect on enzymatic activity and allergenicity is currently under study (*5*). With the possible exception of its behavior toward aggregated substrates, the activity of the bee-venom enzyme is similar to that of other PLA_2s (*6*).

Crystal structures are available for representative Class I and Class II enzymes (*7*, *8*). We report the crystal structure of bee-venom PLA_2 in a complex with a transition-state analogue, $diC_8(2Ph)PE$ (Table 1 and Fig. 1). As expected, the conserved sequence segments of the bee-venom PLA_2 preserve the functional substructures found in Class I/II enzymes but are arranged within a different overall architecture (Fig. 2). The interaction of the inhibitor with the bee-venom enzyme shows how the rate-limiting formation of a putative tetrahedral intermediate is fostered by the enzyme's catalytic components and defines the mechanism by which the hydrophobic alkyl moieties of the phospholipid participate in productive-mode binding.

In Fig. 3 the position of $diC_8(2Ph)PE$ is

D. L. Scott, Z. Otwinowski, P. B. Sigler, Department of Molecular Biophysics and Biochemistry and the Howard Hughes Medical Institute, Yale University, New Haven, CT 06511.
M. H. Gelb, Departments of Chemistry and Biochemistry, University of Washington, Seattle, WA 98195.